Winter-spring warming in the North Atlantic during the last 2,000 years: Evidence from Southwest Iceland

Nora Richter[1,2], James M. Russell[1], Johanna Garfinkel[1], Yongsong Huang[1]

[1] Department of Earth, Environmental and Planetary Sciences, Brown University, Providence, RI 02912, USA

[2] The Josephine Bay Paul Center for Comparative Molecular Biology and Evolution, Marine Biological Laboratory, Woods Hole, MA, 02543, USA

Correspondence to: Nora Richter (nora.richter@nioz.nl)

Abstract. Temperature reconstructions from the Northern Hemisphere (NH) generally indicate cooling over the Holocene which is often attributed to decreasing summer insolation. However, climate model simulations predict that rising atmospheric CO_2 concentrations and the collapse of the Laurentian ice sheet caused mean annual warming during this epoch. This contrast could reflect a seasonal bias in temperature proxies, and particularly a lack of proxies that record cold (late fall-early spring) season temperatures, or inaccuracies in climate model predictions of NH temperature. We reconstructed winter-spring temperatures during the Common Era (i.e. the last 2,000 years) using alkenones, lipids produced by Isochrysidales haptophyte algae that bloom during spring ice-off, preserved in sediments from Vestra Gíslholtsvatn (VGHV), southwest Iceland. Our record indicates cold-season temperatures warmed during the last 2,000 years, in contrast to NH averages. Sensitivity tests with a lake energy balance model show that this warming is likely driven by increasing winter-spring insolation. We also found distinct seasonal differences in centennial-scale, cold-season temperature variations in VGHV compared to existing records of summer and annual temperatures from Iceland. Sustained or abrupt cooling in VGHV temperatures are associated with the cumulative effects of solar minima and volcanic eruptions, and potentially ocean and sea-ice feedbacks associated with cooling in the broader Arctic. However, multi-decadal to centennial-scale changes in winter-spring temperatures were strongly modulated by internal climate variability, i.e. the North Atlantic Oscillation, which can result in winter warming in Iceland even after a major negative radiative perturbation.

1 Introduction

Temperatures in the Northern Hemisphere (NH) are generally thought to have cooled over the past 2,000 years, culminating in the Little Ice Age (LIA, c. 1450-1850 CE) (Kaufman et al., 2009; PAGES 2K Consortium, 2013, 2019; McKay and Kaufman, 2014). However, the majority of NH temperature reconstructions are based on proxies that respond to climate change during the warm season and may not capture trends in annual or winter and spring temperatures (Liu et al., 2014; PAGES 2K Consortium, 2019). This limits our understanding of major atmospheric phenomena in the NH, such as the North Atlantic Oscillation (NAO) which dominates wintertime variability, as well as changes in ocean circulation and other phenomena driving variability in the extent of Arctic sea ice.

Many oceanic and atmospheric processes that influence surface climate in the Atlantic and the broader NH are centered in the high North Atlantic region, making it an important location to study changes during the winter and spring seasons (Hurrell, 1995; Yeager and Robson, 2017). Terrestrial paleoclimate records from Iceland, for instance, have the potential to resolve temperature changes during the winter and spring seasons as this region is sensitive to the NAO and sits near the southern limit of Arctic sea ice (Hurrell, 1995; Hanna et al., 2004, 2006). The high sedimentation rates in Icelandic lakes, along with well-known volcanic eruptions that can be used as age constraints on sediment successions, make this an ideal location and archive to test how winter and spring temperatures evolved over the past 2,000 years (Larsen and Eiríksson, 2008; Geirsdóttir et al., 2009, 2019; Larsen et al., 2011; Langdon et al., 2011; Holmes et al., 2016). However, existing terrestrial records of temperature from Iceland are limited due to their sensitivity to the warm season, low temporal resolution and length, or compounding effects on proxies from human land-use or precipitation over the past 2,000 years.

Here we present a reconstruction of winter-spring temperatures developed using well-dated lake sediments from southwest Iceland to assess seasonal temperature changes in the North Atlantic climate over the past 2,000 years. We take advantage of alkenone-production by Group I Isochrysidales (i.e. haptophyte algae) during the spring season to develop a record of winter-spring temperatures and investigate the forcings responsible for cold-season temperature changes using a lake energy balance model.

2 Methods

2.1 Study site and age model

Vestra Gíslholtsvatn (VGHV) is a small lake (1.57 km^2) located in southwest Iceland (61 m a.s.l., 63° 56′ N, 20° 31′ W; Fig. 1), about 25 km from the coast (Blair et al., 2015). Mean monthly temperatures range from -1.4 °C during the winter months (DJF) to 10.4 °C during the summer months (JJA) (station at Hella, 1958-2005 CE; Icelandic Meteorological Office). Cores

2

were collected in 2008 using a Bolivia piston coring system (Blair et al., 2015), and were sampled at the National Lacustrine Core Facility (LacCore) at the University of Minnesota.

60

The VGHV cores were dated using previously identified tephra, including seven historical and four pre-historical tephra beds (Blair et al., 2015 and references therein). The age model was developed using 'classical' age modeling (CLAM) with a smoothed spline fit. The resulting age model has an uncertainty of 5 to 15 yrs from -50 to 1200 yrs BP and 18 to 83 yrs from 1201 to 2000 yrs BP (Fig. 2; Blaauw, 2010).
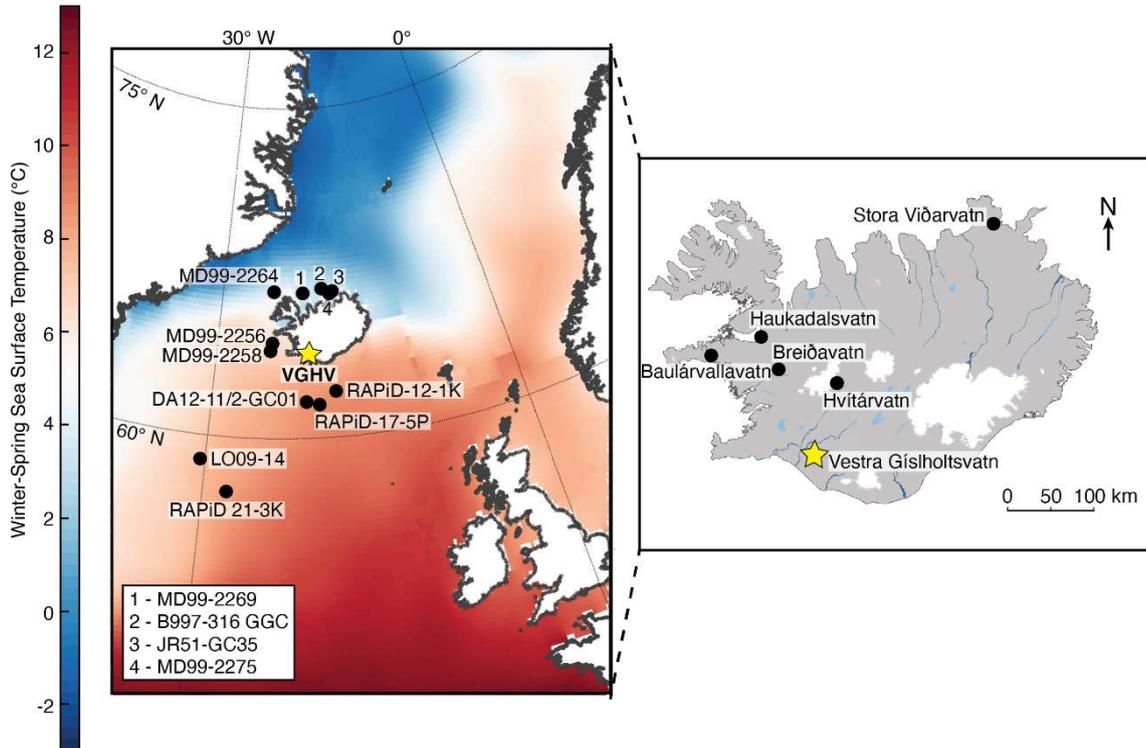
65

Figure 1. Map of mean winter-spring (DJFMAM) sea surface temperatures from 1955-2017 in the high North Atlantic region. The marine sediment cores MD99-2269 (Moros et al., 2006; Justwan et al., 2008; Cabedo-Sanz et al., 2016), B997-316 GGC (Harning et al., 2019), JR51-GC35 (Cabedo-Sanz et al., 2016), MD99-2275 (Jiang et al., 2005, 2015; Massé et al., 2008; Sicre et al., 2008; Ran et al., 2011), MD99-2264 (Ólafsdóttir et al., 2010), MD99-2256 (Ólafsdóttir et al., 2010), MD99-2258 (Axford et al., 2011), DA12-11/2-GC01 (Orme et al., 2018; Van Nieuwenhove et al., 2018), RAPiD-12-1K (Thornalley et al., 2009), RAPiD-17-5P (Moffa-Sánchez et al., 2014), LO09-14 (Berner et al., 2008), and RAPiD 21-3K (Sicre et al., 2011; Miettinen et al., 2012) that are discussed in the text are indicated. The the locations of lake sediment records from Stora Viðarvatn (Axford et al., 2009), Haukadalsvatn (Geirsdóttir et al., 2009), Baulárvallavatn (Holmes et al., 2016), Breiðavatn (Gathorne-Hardy et al., 2009), and Hvítárvatn (Larsen et al., 2011) are indicated. The study site, Vestra Gíslholtsvatn (VGHV), is marked by a yellow star. The maps were made using data from Natural Earth, the National Land Survey of Iceland, and the National Oceanic and Atmospheric Administration (NOAA) World Ocean Database (Boyer et al., 2018).

3

2.2 Lipid analyses

Sediments were freeze-dried and extracted using a Dionex^{TM} accelerated solvent extraction (ASE 350) system at 120 °C and
1200 psi. All of the extracts were separated by silica gel (40-63 μm, 60 Å) flash chromatography to obtain alkane (hexane; Hex), ketone (dichloromethane; DCM), and polar (methanol; MeOH) fractions. Saponification was used to remove wax esters by dissolving the dried ketone fraction in a 1 molar potassium hydroxide solution with MeOH:H$_2$O (95:5, v/v) and heating the samples for 3 hrs at 65 °C. 5 % NaCl in H$_2$O and 50 % HCl in H$_2$O were added to the samples and the lipid faction was extracted using Hex (100 %). Ketone fractions were further purified using silver nitrate columns (D'Andrea et al., 2007) with DCM (100 %) followed by ethyl acetate (100 %) to elute the alkenones. If additional cleaning was needed, a modified procedure from Salacup et al. (2019) was used. The alkenone fraction was dried under N$_2$ gas and re-dissolved in 1.5 mL of DCM:Hex (2:1, v/v). To this, a 1.5 mL solution of 100 mg/mL urea in MeOH was added. The resulting crystals were dried under N$_2$ gas, and the urea addition was repeated two more times. The dried urea crystals were cleaned with Hex (100 %) and extracted as the non-adduct. Milli-Q water was added to the vial to fully dissolve the urea crystals, and the adduct was extracted using Hex (100 %). The samples were then analyzed for alkenones. For several samples, co-eluting compounds were still present, or concentrations were too low for reliable quantification. These samples were not included in our final reconstruction.
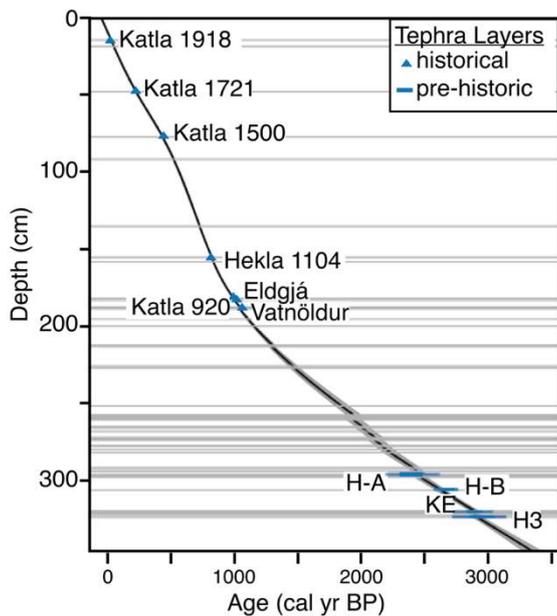
Figure 2. Age model for Vestra Gíslholtsvatn with historic and pre-historic tephra layers (previously identified by Blair et al., 2015 and references therein) used for dating indicated. The gray lines represent tephra layers that were removed from the age model.

4

The resulting alkenone fraction was analyzed using an Agilent 6890N gas chromatography (GC) and flame ionization detector (FID) system with an Agilent VF-200ms capillary column (60 m x 250 µm x 0.10 µm). Samples were injected into a CIS-PTV inlet in solvent vent mode (6.9 psi at 112 °C). The oven program was set to 50 °C and increased to 235 °C at 20 °C/min and ramped to 320 °C at 1.39 °C/min where it was held isothermally for 5 min. For additional verification or identification of co-eluting compounds, samples were run on an Agilent 6890N GC system coupled with an Agilent 5793 N quadrupole mass spectrometer (MS). All samples were injected with pulsed splitless injection mode (20 psi at 315 °C) and run on an Agilent VF-200ms capillary column (60 m x 250 µm x 0.10 µm). The oven program was started at 40 °C for 1 min, ramped up to 255 °C at 20 °C/min, increased again to 315 °C at 2 °C/min, and then held isothermally for 10 min. The MS ionization energy was set to 70 eV with a scan range of 50 to 600 *m/z*.

2.3 Alkenones as a proxy for lake water temperatures

Alkenones are long-chain ketones produced by Isochrysidales haptophyte algae in both marine and lacustrine environments. Numerous marine-based culture and core-top studies show that variations in alkenone saturation (i.e., changes in $C_{37:3}Me$ and $C_{37:2}Me$ production) are inversely correlated with temperature, and can be linearly calibrated to temperature using either the U_{37}^{K} or $U_{37}^{K'}$ index (Brassell et al., 1986; Prahl and Wakeham, 1987; Prahl et al., 1988; Müller et al., 1998; Conte et al., 2006). Similarly, culture studies, core tops, and in situ measurements in lakes show that changes in alkenone saturation are also correlated with temperature (Zink et al., 2001; Sun et al., 2007; Toney et al., 2010; D'Andrea et al., 2011, 2012, 2016; Wang and Liu, 2013; Nakamura et al., 2014; Longo et al., 2016, 2018; Zheng et al., 2016). The U_{37}^{K} index can be applied to lacustrine environments and is calculated as follows:

$$U_{37}^{K} = \frac{[C_{37:2}Me] - [C_{37:4}Me]}{[C_{37:2}Me] + [C_{37:3}Me] + [C_{37:3*}Me] + [C_{37:4}Me]} \qquad (1)$$

Sedimentary alkenones may derive from multiple alkenone-producing species, mainly Group I and II Isochrysidales, with distinct alkenone signatures and varying responses to temperature (Coolen et al., 2004; Sun et al., 2007; Theroux et al., 2010, 2013; Ono et al., 2012; Toney et al., 2012; Nakamura et al., 2014; D'Andrea et al., 2016). Group I Isochrysidales produces distinct tri-unsaturated alkenones (e.g., $C_{37:3*}Me$), which can be used to test for species-mixing effects with the RIK_{37} index (Longo et al., 2016):

$$RIK_{37} = \frac{[C_{37:3}]}{[C_{37:3} + C_{37:3*}]} \qquad (2)$$

A RIK_{37} value of 1.0 suggests a predominance of the $C_{37:3}Me$ and the presence of Group II Isochrysidales, while values from 0.48 to 0.63 are empirically shown to correspond to Group I Isochrysidales (Longo et al., 2016, 2018).

5

Group I Isochrysidales and their corresponding alkenones have, so far, only been identified in Northern Hemisphere lakes at latitudes ranging from 42-81 °N (Longo et al., 2018; Richter et al., 2019). The Northern Hemisphere lake calibration for Group I alkenones, which includes VGHV, was developed using the average spring temperatures for each lake during ice-off and the main Group I Isochrysidales bloom ($U_{37}^K = 0.029T$-0.49, $r^2 = 0.60$, RMSE = ± 1.69°C; Longo et al., 2018). An updated calibration for Group I that includes additional lakes in northeastern China ($U_{37}^K = 0.030T$-0.479, $r^2 = 0.0479$) has an RMSE = ± 1.71°C (Yao et al., 2019). Group I alkenone calibrations also exist for Lake BrayaSø in Greenland ($U_{37}^K = 0.0245T$-0.779, $r^2 = 0.96$, note the calibration also includes data from several German lakes, see Zink et al., 2001; D'Andrea et al., 2011), Lake Kongressvatnet in Svalbard ($U_{37}^K = 0.0255T$-0.804, $r^2 = 0.85$, D'Andrea et al., 2012), Toolik Lake in Alaska ($U_{37}^K = 0.021T$-0.68, $r^2 = 0.85$; Longo et al., 2016), and Vikvatnet in Norway ($U_{37}^K = 0.0284T$-0.655, $r^2 = 0.94$; D'Andrea et al., 2016). Temperature calibrations using the U_{37}^K index were successfully applied to develop high resolution records of summer temperatures in Greenland (c. 5,600 yrs BP; D'Andrea et al., 2011) and Svalbard (1,800 yrs BP; D'Andrea et al., 2012) and a winter-spring temperature record in Alaska (16,000 yrs BP; Longo et al., 2020). However, regional variability in the relationship between the U_{37}^K index and temperature requires the development of local temperature calibrations (Wang and Liu, 2013; D'Andrea et al., 2016; Longo et al., 2016). Unfortunately, there is currently no local calibration for Icelandic lakes.

2.4 Seasonal temperature sensitivity of Group I alkenones in lakes

In Greenland and Alaska, Group I Isochrysidales bloom during the early spring in the photic zone as lake ice starts to melt (D'Andrea and Huang, 2005; D'Andrea et al., 2011; Longo et al., 2016, 2018). Alkenone production starts prior to ice-off, then increases as the lake undergoes isothermal mixing, and decreases when thermal stratification begins to develop in late spring/early summer (Longo et al., 2018). This holds true for other Group I-containing lakes in the NH, including lakes in Iceland, as evidenced by the positive correlation between the U_{37}^K index and mean spring air temperatures (Longo et al., 2018).

We investigated the controls on spring lake water temperatures and the timing of ice-melt in VGHV using a lake energy balance model (Dee et al., 2018). The purpose of the lake model was to determine the sensitivity of our proxy to different forcing mechanisms by assessing the magnitude of the temperature response and timing of ice-melt relative to our control simulation. The model was initialized using ERA-Interim daily data (1979-2018 CE; ECMWF; Dee et al., 2011) averaged over grid cells covering southwest Iceland (18.25° W-22.75° W by 63.00° N-64.50° N for a 0.75° x 0.75° grid). An initial control simulation was run for 39 years, followed by sensitivity tests where various perturbations were introduced.

The perturbation experiments focused on the effects of changes in seasonal air temperatures and shortwave and longwave radiation on lake surface temperatures and ice-off dates. We used instrumental data from Hella, Iceland (1958-2005 CE) to determine the magnitude of seasonal air temperature changes (Icelandic Meteorological Office). Between 1958-2004 the range of mean seasonal temperatures are as follows: winter (DJF) -3.7 °C to 1.8 °C, spring (MAM) -1.0 °C to 6.9 °C, summer (JJA)

6

8.8 °C to 12.0 °C, and fall (SON) -1.3 °C to 6.7 °C. To constrain the seasonality of our proxy, we perturbed the ERA interim seasonal air temperature values by -7 °C, -3 °C, 0 °C, +3 °C, and +7 °C and re-ran the lake model with the adjusted parameters. We repeated these experiments, but instead perturbed surface incident shortwave radiation to test how external forcings can drive changes in temperature. Incoming (top of the atmosphere) insolation at 63 °N has increased in winter (DJF) by 1.5 W m^{-2} and in spring (MAM) by 3.7 W m^{-2} over the past 2,000 years (Laskar et al., 2004). We therefore tested insolation forcing by perturbing seasonal changes in surface incident shortwave radiation by -4 W m^{-2}, -2 W m^{-2}, 0 W m^{-2}, +2 W m^{-2}, and +4 W m^{-2}. The effects of volcanic eruptions on temperature and ice-off dates were also tested by changing shortwave radiation by -30 W m^{-2}, -10 W m^{-2}, 0 W m^{-2}, +10 W m^{-2}, and +30 W m^{-2}. These values were based on regional radiative feedback studies from the 1783 CE Laki (Oman et al., 2006) and 2010 CE Eyjafjallajökull (Hirtl et al., 2019) eruptions in Iceland. It should be noted that Iceland receives minimal light during the winter months and VGHV is frozen during the winter months, so we expect little to no direct influence of insolation on lake water temperatures during winter. Shortwave radiation values for the winter (DJF) were set to 0 W m^{-2} if a negative perturbation decreased shortwave radiation below 0 W m^{-2}. To assess the effects of longwave radiation on lake water temperatures and ice-off dates, we decreased and increased incoming longwave radiation by -0.2 W m^{-2}, 0 W m^{-2}, +0.2 W m^{-2}. These values reflect the forcing from well-mixed greenhouse gas (GHG) radiation during the pre-industrial period (Schmidt et al., 2011).

3 Results

3.1 U^K_{37} index: corrections for species-mixing

Our U^K_{37} index from VGHV suggests that there was substantial variability in temperature during the last 2,000 years, but there was also variability in the community of alkenone-producers (Fig. 3a). Alkenones in VGHV surface sediments have a RIK_{37} value of 0.60 and genetic analyses confirm that Group I Isochrysidales is the main alkenone-producer (Longo et al., 2018; Richter et al., 2019). However, the RIK_{37} values increase slightly above the Group I cut-off of 0.63 about c. 500 CE, and then show a more sustained increase after human settlement in Iceland (c. 870 CE), suggesting that Group II alkenone-producers were also present in the lake (Fig. 3b).
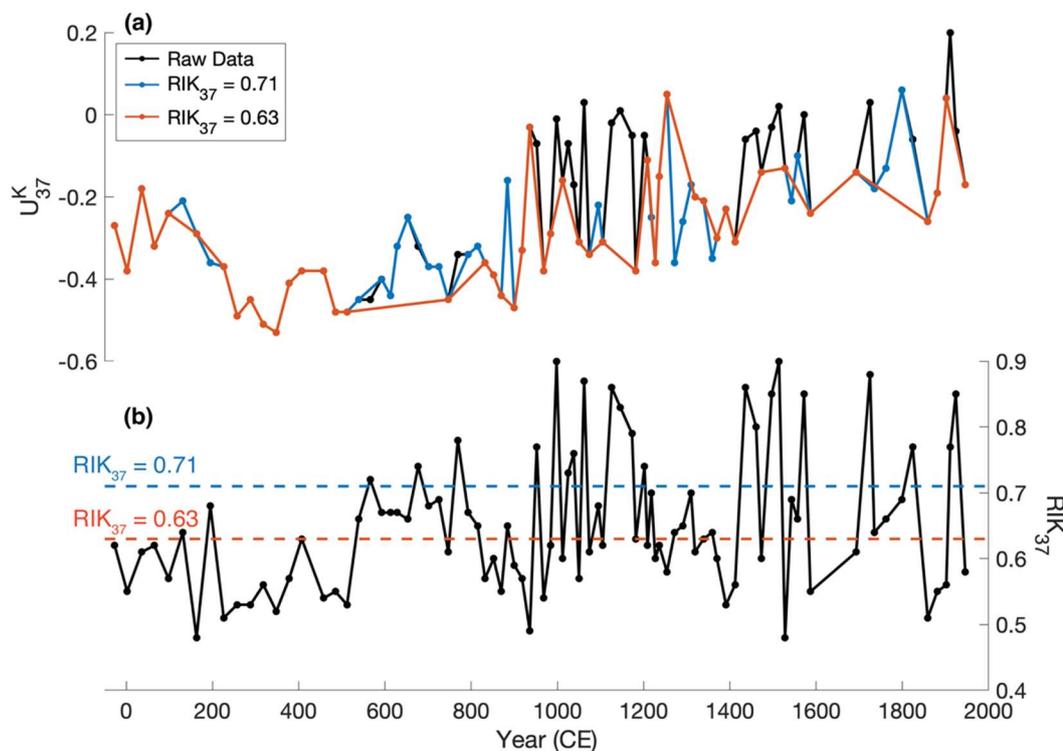
Figure 3. (a) The raw data for the U_{37}^{K} index is indicated in black, and the corrected U_{37}^{K} index with a RIK$_{37}$ cut-off of 0.63 and 0.71 are shown in orange and blue, respectively. (b) The original RIK$_{37}$ index is shown below for comparison with the empirical cut-off, RIK$_{37}$ = 0.63, and cut-off for RIK$_{37}$ = 0.71 indicated.

To evaluate the potential impacts of species mixing on the U_{37}^{K} record, samples with a high abundance of Group II alkenones were removed. We tested several different cut-offs for the RIK$_{37}$ index and compared changes in the mean U_{37}^{K} values (Fig. 4). If no correction is applied (RIK$_{37}$ = 1.0), then U_{37}^{K} = -0.34 ± 0.12 from 0-1000 CE and U_{37}^{K}= -0.14 ± 0.13 from 1001-2000 CE. The empirically defined cut-off of 0.63 yields a mean U_{37}^{K} index of -0.37 ± 0.12 from 0-1000 CE and -0.20 ± 0.10 from 1001-2000 CE. A less stringent RIK$_{37}$ cut-off at 0.71, results in no significant difference in the mean or the variability of the data (0-1000 CE U_{37}^{K} = -0.36 ± 0.10 and 1001-2000 CE U_{37}^{K} = -0.21 ± 0.11). Species mixing thus affects the U_{37}^{K} temperature record, but regardless of the correction applied to the data, there is an increase in the mean U_{37}^{K} values (which we interpret as warming) from 0-1000 CE to 1001-2000 CE.

Using a RIK$_{37}$ cut-off of 0.71, the corrected U_{37}^{K} values and RIK$_{37}$ index are not correlated (r = 0.11, p = 0.35), indicating that species-mixing effects do not affect the final temperature calibration. The resulting U_{37}^{K} values can be interpreted as a record of temperature changes from Group I alkenones.

8
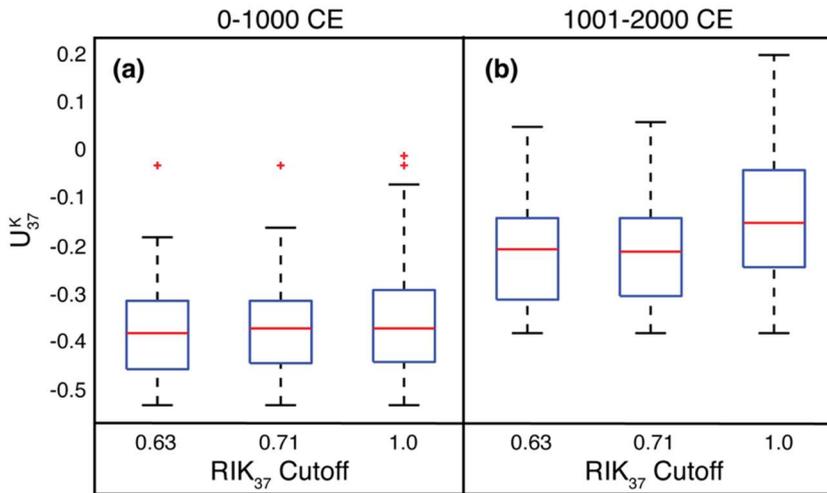
Figure 4. Different RIK$_{37}$ cutoffs applied to the U$_{37}^K$ index for (a) 0-1000 CE and (b) 1001-2000 CE. A RIK$_{37}$ value of 1.0 indicates that the data was not corrected for species-mixing effects, while RIK$_{37}$ = 0.63 corresponds to the empirically defined cut-off for Group I and II (Longo et al., 2018).

3.2 Controls on spring lake water temperature

Results from the lake energy balance model show that seasonal perturbations can have a strong influence on spring lake water temperatures and ice-off dates in VGHV (Fig. 5, Tables S1 and S3). The control run yields an average ice-off date of April 15th with water temperatures on May 1st about 6.6 °C. Air temperature perturbations during the winter (DJF) and spring (MAM) alter the timing of ice-off and how rapidly surface water temperatures warm, with warmer air temperatures leading to warmer water temperatures and earlier ice-off dates (Fig. 5a-b). In addition, an increase in shortwave solar radiation during the spring season (MAM) leads to earlier ice-off dates and warmer lake water temperatures (Fig. 5c-d, Table A2). Shorter days during the winter months (DJF) limits the amount of shortwave radiation reaching Iceland, and therefore has a minimal influence on Icelandic temperatures (Fig. 5d and f). Shortwave radiative perturbations from volcanic eruptions during the winter season result in small changes in spring lake water temperatures and ice-off dates, while eruptions during the spring lead to much colder spring water temperatures and later ice-off dates (Fig. 5e-f, Table A2). There are no competing effects of summer (JJA) or fall (SON) insolation and air temperature on spring lake water temperatures and the timing of ice-out. The increase in longwave radiation from GHGs during the pre-industrial period is relatively small and has no significant influence on either lake water temperatures (change from control = 0.01 ± 1.02 °C) or ice-off dates (change from control = -0.03 ± 8.77 days; Fig. A1, Table A3). Thus, the timing of the alkenone bloom and the water temperatures recorded by the alkenones are most likely responses to changes in air temperature and temperature changes driven by shortwave radiation during the late winter and spring season.

9
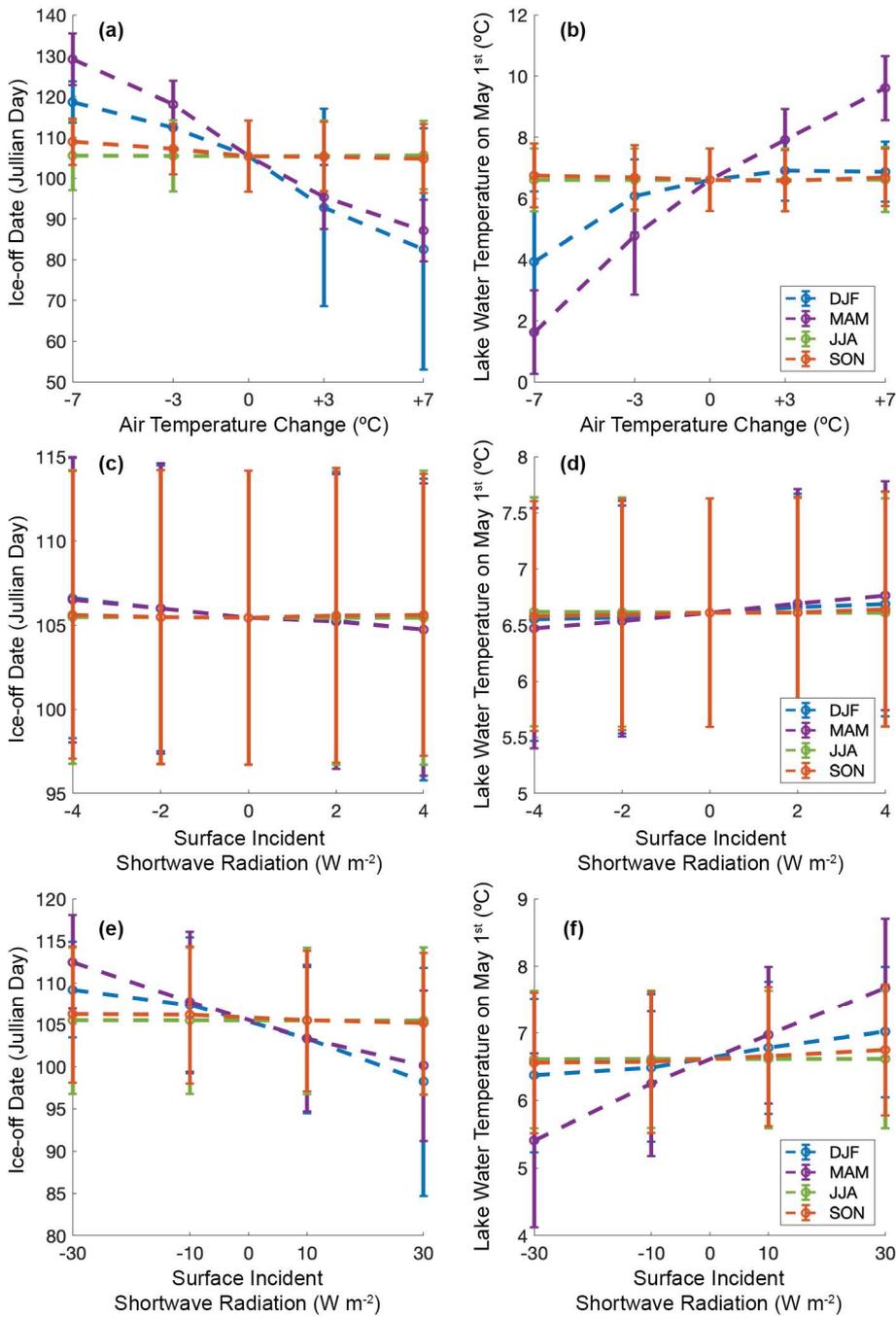
Figure 5. Lake model sensitivity tests showing the impacts of air temperature perturbations during different seasons on (a) ice-off dates and (b) lake water temperatures on May 1st. Similarly, the results for shortwave radiation perturbations that reflect changes in orbital insolation during different seasons for (c) ice-off dates and (d) lake water temperatures and changes from volcanic

eruptions for (e) ice-off dates and (f) lake water temperatures are shown. Seasonal changes are shown for winter (DJF, blue), spring (MAM, purple), summer (JJA, green), and fall (SON, orange).

3.3 Long-term trends and short-term variability in the U_{37}^K record and temperature

The U_{37}^K index can provide temperature estimates using linear relationships that are calibrated in lakes with Group I alkenone-producers (D'Andrea et al. 2011, 2016; Longo et al., 2016, 2018). Existing temperature calibrations, except for the Northern Hemisphere calibration by Longo et al. (2018), for Group I are site-specific and therefore cannot be readily applied to VGHV (e.g. calibrations give estimates of 10.2 to 33.5 °C (D'Andrea et al., 2011), 7.1 to 34.4 °C (Longo et al., 2016), 4.4 to 24.5 °C (D'Andrea et al., 2016), -1.4 to 18.3 °C (calibration for Northern Hemisphere lakes by Longo et al., 2018; see Fig. A2). Most of the variation between sites is accounted for by the y-intercept of the calibration, so the slope of Group I calibrations was suggested as a better determinant of relative temperature changes for sites lacking a site-specific calibration (D'Andrea et al., 2016). However, the slopes determined for Group I calibrations still result in a very large and likely unreasonable temperature range of 26.9 °C for $U_{37}^K = 0.0219T$ (D'Andrea et al., 2016). The slope determined for Group III alkenone calibrations ($U_{37}^K = 0.0447T$; D'Andrea et al., 2016) provides a more reasonable temperature range of 13.2 °C and an estimated temperature change of 8 °C from 250-350 CE to 1850-1950 CE. Given the sensitivity of VGHV lake water temperatures to winter and spring season perturbations and the large variability in winter and spring temperatures observed in the instrumental data (mean temperatures in the winter and spring (DJFMAM) season range from -2.4 °C to 3.4 °C with a seasonal variance of 13.1 °C between 1958-2004 at Hella station; Icelandic Meteorological Office), it is plausible to observe temperature swings close to 10 °C during the spring transitional season (Fig. 5b). However, the amplitude of reconstructed temperatures is still relatively large considering that each sample is an average of 5-19 years, and most likely stems from the lack of a local calibration. Nevertheless, the U_{37}^K index is known to be highly sensitive to temperatures in NH lakes, therefore we use the U_{37}^K index to infer and evaluate qualitative changes in temperature trends and variability during the past 2,000 years.

The U_{37}^K record from VGHV, corrected for species mixing, exhibits a long-term trend towards warmer spring lake water temperatures over the last 2,000 years as well as strong multi-decadal to centennial variability (Fig. 6). The gradual warming trend in our record begins after c. 400 CE. In particular, a warmer period occurs from the start of our record to c. 200 CE, followed by cooling from c. 250-600 CE. Temperature variability increases after c. 850 CE, and warmer periods occur between c. 850-1050 CE, c. 1100-1300 CE, and c. 1450-1550 CE. Relatively cooler periods occur at c. 1100-1200 CE, c. 1300-1450 CE, c. 1550-1750 CE, and c. 1850-1880 CE. However, caution should be used when interpreting results after c. 1400 CE because of low sampling resolution (c. 50 yrs between each sample).

4 Discussion

4.1 Long-term seasonal climate trends in North Atlantic paleoclimate records

11

Mean annual temperature syntheses from the NH exhibit a long-term cooling trend over the last 2,000 years (Kaufman et al., 2009; PAGES 2K Consortium, 2013, 2019) that is often interpreted as a response to decreasing summer insolation (Kaufman et al., 2009) and/or increased volcanic activity during the LIA (Miller et al., 2012). Climate model simulations suggest that solar variability acts as a secondary source of variability and land use changes may be important for explaining some of the changes in NH surface temperatures between the MCA and LIA, whereas increases in greenhouse gases remain stable until the late 19th century (Otto-Bliesner et al., 2016). The magnitude of the cooling trend and centennial and multi-decadal changes differs among global temperature reconstructions (PAGES 2K Consortium, 2019) and is often larger in NH temperature reconstructions compared to climate model simulations (Rehfeld et al., 2016; Ljungqvist et al., 2019). The discrepancies in temperature reconstructions and climate models could stem from a warm season bias in NH proxy reconstructions, leading to an overestimation of changes in mean annual and cold season temperatures in proxy reconstructions compared to climate model simulations (Liu et al., 2014; Rehfeld et al., 2016; PAGES 2K Consortium, 2019).

Winter-spring temperatures from VGHV warm over the past 2,000 years (Fig. 6), and our lake energy balance modelling results indicate that increasing shortwave radiation and air temperatures during the winter and spring season could result in warmer water temperatures and earlier ice-off dates. Lake water temperatures in VGHV solely respond to changes during the winter and spring season because the lake re-freezes every winter and reaches minimum lake water temperatures, meaning any influence from the previous summer or fall season are negligible (e.g. Assel and Robertson, 1995). Mean annual long-wave radiative forcing, i.e. GHGs, over the pre-industrial period has a minimal influence on water temperatures and ice-off dates. This suggests that the long-term warming trend in VGHV is driven by air temperature changes and solar insolation during the winter and spring season. However, as our record only spans the last 2,000 years, the warming trend in our record could also be a feature of the last millennium associated with regional processes.

Iceland has a maritime climate and also sits near the edge of the Arctic sea ice; therefore, air temperatures are sensitive to regional sea-ice feedbacks and variations in sea surface temperatures (SSTs). The VGHV temperature record shows that winter and spring air temperatures warmed over the last millennium, whereas temperature and sea ice reconstructions suggest that summer air temperatures cooled in Northern and Western Iceland as sea ice increased with the coldest period occurring during the 18th and 19th centuries (Ogilvie and Jónsson, 2001; Moros et al., 2006; Massé et al., 2008; Gathorne-Hardy et al., 2009; Axford et al., 2009, 2011; Langdon et al., 2011; Cabedo-Sanz et al., 2016; Holmes et al., 2016). Paleo- and historical records, however, indicate that sea ice was only present along the southern and western coasts of Iceland, where our study site VGHV is located, during severe ice years when sea ice is advected clockwise around the country (Ogilvie, 1996; Axford et al., 2011; Cabedo-Sanz et al., 2016). Similarly, millennial-scale changes in spring temperatures inferred from biogenic silica in western Iceland are decoupled from temperature and sea-ice changes in Northern Iceland, suggesting that spring temperatures are likely more sensitive to changes in regional SSTs (Geirsdóttir et al., 2009). SST reconstructions near southern Iceland show that surface temperatures either increased (Berner et al., 2008; Thornalley et al., 2009; Miettinen et al., 2012; Orme et al., 2018) or

did not significantly change (Sicre et al., 2011; Van Nieuwenhove et al., 2018) over the last 2,000 years. Marine reconstructions of temperature from below the summer thermocline and bottom water record a decrease in mean annual temperatures over the Common Era (Thornalley et al., 2009; Ólafsdóttir et al., 2010; Moffa-Sánchez et al., 2014) as the transport of warm North Atlantic Current waters by the Irminger Current decreased over the last 2,000 years (Ólafsdóttir et al., 2010). Based on existing paleo- and historical records we conclude that sea ice feedbacks only play a minor role in driving long-term changes in winter and spring temperatures at our study site, whereas an increase in SSTs along the southern coast could contribute to the warming trend observed in our record. However, discrepancies in existing proxy records makes it difficult to correlate changes in SSTs to changes in winter and spring temperatures at VGHV.

Long-term warming trends over the Holocene and the Common Era were also observed in other records of cold-season temperatures in the NH. For instance, pollen records of cold-season temperatures from North America and Europe (Mauri et al., 2015; Marsicek et al., 2018) and an alkenone reconstruction of winter-spring temperatures from Alaska (Longo et al., 2020) suggest that increasing winter and spring orbital insolation over the Holocene drove warming during the winter and spring season. Winter warming over the Holocene, including the Common Era, was also inferred from chrysophyte cysts in Spain (Pla and Catalan, 2005), ice-wedge records in the Siberian Arctic (Meyer et al., 2015; Opel et al., 2017), and a speleothem record from the Ural Mountains in Russia (Baker et al., 2017). A marine record directly south of Iceland from the North Atlantic subpolar gyre, records winter SSTs that are on average warmer over the last 2,000 years relative to the early to mid-Holocene (Van Nieuwenhove et al., 2018). In each of these studies, insolation and/or rising greenhouse gases are proposed as the primary mechanisms driving changes in seasonal temperatures, supporting the results of our energy balance model.

Although there are existing reconstructions of NH winter and spring temperatures during the Common Era, the high-resolution reconstruction of winter-spring temperatures from VGHV is one of the few sites in the Northern high latitudes where the effects of seasonal insolation on winter temperature can be tested without having to account for the influence of confounding factors, such as precipitation, on proxy records. For instance, varve thickness records have been interpreted to reflect winter temperatures but might be influenced by human activities in the catchment area, variations in snow accumulation, the timing of spring melt, and changes in precipitation (Ojala and Alenius, 2005; Haltia-Hovi et al., 2007). Varve thickness records from the Arctic that record changes in snow or glacial melt are also used to infer long-term cooling during the melt season; however, the melt season in the high Arctic often extends well into the summer months (Cook et al., 2009; Larsen et al., 2011) and can be affected by Arctic summer hydrology. Water isotope records from ice cores from Svalbard and a stalagmite from the Central Alps are sensitive to winter air temperatures during the instrumental period, but changes in the moisture source and seasonality of precipitation over time can alter long-term temperature interpretations (Isaksson et al., 2005; Mangini et al., 2005; Divine et al., 2011a, b). Although our record lacks a local calibration, we argue that the U_{37}^{K} record from VGHV provides a robust, albeit qualitative, record of winter-spring temperatures given the unique seasonal growth ecology of Group I haptophytes in NH lakes.

13
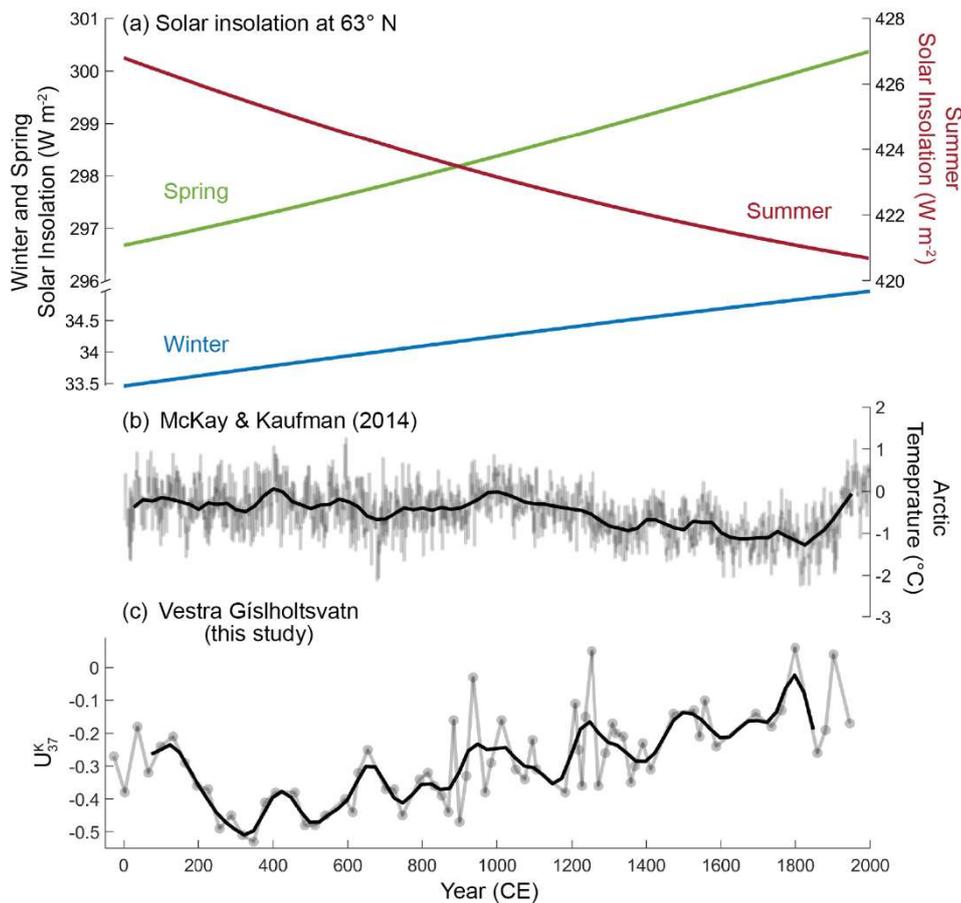
Figure 6. (a) Changes in solar insolation at 63°N for winter (DJF), spring (MAM), and summer (JJA) are shown for the past 2,000
330 **years (Laskar et al., 2004). In addition, (b) a compilation of Arctic temperature reconstructions (McKay and Kaufman, 2014) is**
shown for comparison with the (e) winter-spring temperature reconstruction from VGHV (the thick black lines for panels (b) and
(c) are lowpass filters with data resampled to every 25 years to capture the low-frequency variability of the datasets).

The warming trend observed in our new record from Iceland and other records of cold-season temperatures from the NH
335 suggest that long-term temperature changes are driven by a common forcing, orbitally-driven changes in winter and spring
insolation, during the Holocene (Mauri et al., 2015; Meyer et al., 2015; Baker et al., 2017; Marsicek et al., 2018; Van
Nieuwenhove et al., 2018; Longo et al., 2020) and during the Common Era (Pla and Catalan, 2005; Meyer et al., 2015; Baker
et al., 2017; Opel et al., 2017). Our lake model results confirm that water temperatures are sensitive to seasonal air temperatures
and indirectly respond to perturbations in shortwave radiation, indicating that the long-term warming trend observed in the
340 VGHV record can in part be attributed to increasing late winter and early spring insolation.

14

4.2 Seasonal multi-decadal to centennial climate variability in the North Atlantic

The VGHV reconstruction of winter-spring temperatures provides an opportunity to test how changes in internal climate variability and external forcings (volcanic eruptions and total solar irradiance, or TSI) influence temperature changes during the winter and spring seasons in the North Atlantic region. This is important for understanding multi-decadal to centennial climate changes during the winter and spring seasons and the role of the Atlantic Multi-decadal Variability/Oscillation (AMV/AMO), a low-frequency basin-wide North Atlantic SST anomaly that varies in response to external forcings and internal variability, in driving and/or responding to changes during the winter (Kerr, 2000; Wang et al., 2017; Yeager and Robson, 2017). The NAO, defined by differences in sea-level pressure between the subpolar low and the subtropical high, is a major source of atmospheric variability during the winter months (Hurrell, 1995). Although the NAO is mainly associated with interannual timescales, there is also evidence that NAO-like patterns can emerge at multi-annual to centennial timescales, potentially linked to coupled changes in oceanic and atmospheric circulation (Visbeck et al., 2003; Delworth et al., 2016; Yeager and Robson 2017). For instance, a positive (negative) NAO phase that persists for multiple winters can lead to increased (decreased) deepwater formation in the Labrador Sea and strengthening (weakening) of the subpolar gyre and the meridional overturning circulation, thereby resulting in an increased (decreased) transport of warm waters towards the poles (Eden and Jung, 2001; Visbeck et al., 2003; Latif et al., 2006). Alternatively, an increase in the southward transport of polar waters could also result in a reduction of deepwater formation in the Labrador Sea and a weaker subpolar gyre, leading to a decrease in northward oceanic heat transport and centennial cooling of ocean and regional air temperatures (Moffa-Sánchez and Hall, 2017; Moreno-Chamarro et al., 2017).

Whether forced or unforced, variability in winter atmospheric circulation, including the NAO, and sea ice extent are often linked to multi-decadal and centennial climate change in the North Atlantic region, particularly over Iceland (e.g. Hanna et al., 2006; Massé et al., 2008; Wang et al., 2017; Yeager and Robson, 2017). In the VGHV record of winter-spring temperatures there is a sharp decrease in the U_{37}^K index c. 250 CE and a corresponding increase in drift ice along the North Icelandic shelf (c. 400-900 CE), which coincides with the Roman Warm Period to Dark Ages Cold Period (DACP) transition (Fig. 7; Cabedo-Sanz et al., 2016). Cooling during the DACP is typically attributed to volcanic eruptions and a minimum in solar activity (c. 400-700 CE; Fig. 7a-b); however, the DACP was not uniform across the NH and records differ as to when peak cooling occurred (Helama et al., 2017). For instance, there is no distinct or prolonged cooling in Iceland SST records during the DACP (Fig. 7c and d; Sicre et al., 2008, 2011; Miettinen et al., 2012; Jiang et al., 2015) or in summer temperature records from Icelandic lakes (Gathorne-Hardy et al., 2009; Axford et al., 2009). In contrast, terrestrial records from the Arctic and Northern Europe indicate that temperatures were on average cooler between c. 450-700 CE and c. 500-650 CE, respectively (Kaufman et al., 2009; Sigl et al., 2015; Helama et al., 2017). A peak in sea ice is also recorded in a high-resolution IP_{25} reconstruction from the North Icelandic shelf (Cabedo-Sanz et al., 2016), whereas lower resolution records that were developed using quartz and IP_{25} show a gradual increase in sea ice after c. 400 CE but not distinct peak (Moros et al., 2006; Cabedo-Sanz et al., 2016).

15

Increases in sea ice during this time period are attributed to a southward shift of the subpolar front and the increased advection of drift ice from Greenland to Northern Iceland (Moros et al., 2006; Cabedo-Sanz et al., 2016), leading to cooler winter and spring temperatures in Northern and Southern Iceland.

Winter and spring temperatures in VGHV were on average higher between c. 880-1100 CE than temperatures during the DACP but were not stable or particularly warm, unlike the climate usually associated with the Norse settlement of Iceland between c. 870-1100 CE (Fig. 7; Ogilvie et al., 2000). This time period corresponds to a peak in TSI and weak volcanic activity (PAGES 2K Consortium, 2013), which could have triggered a positive phase in the AMV/AMO (Otto-Bliesner et al., 2016; Wang et al., 2017) and warmer summer and annual SSTs near Iceland (Sicre et al., 2008, 2011; Justwan et al., 2008; Ran et al., 2011). Summer temperature reconstructions from lakes in Northern and Western Iceland also record warmer temperatures c. 800-1300 CE but with distinct cold excursions occurring between c. 1000-1300 CE (Axford et al., 2009; Gathorne-Hardy et al., 2009; Holmes et al., 2016). Peaks in sea ice, however, are only noted after c. 1200 CE (Ogilvie, 1992; Ogilvie and Jónsson, 2001; Massé et al., 2008; Cabedo-Sanz et al., 2016), suggesting that an alternative mechanism, such as the NAO, may be responsible for the short-term variability observed in terrestrial temperature records from Iceland during this time period.

The 14th-15th centuries mark the start of the LIA and are often associated with a colder-than-average climate in Iceland (Ogilvie, 1984; Ogilvie and Jónsson, 2001). In contrast, the VGHV record indicates there was no prolonged cold period during the winter and spring season between c. 1300-1800 CE. Rather, temperatures inferred from the VGHV record varied on multi-decadal to centennial timescales. Cooling during this time period is associated with major volcanic eruptions and decreases in TSI (PAGES 2K Consortium, 2013; Otto-Bliesner et al., 2016) that most likely resulted in a negative AMV/AMO phase (Wang et al., 2017) and temporary increases in sea ice (Fig. 7; Moros et al., 2006; Massé et al., 2008; Cabedo-Sanz et al., 2016). In marine records from the North Icelandic shelf, this led to cooling of summer/annual SSTs between c. 1400-1900 CE (Fig. 7c and e; Jiang et al., 2005, 2015; Sicre et al., 2008; Ran et al., 2011). A record of subsurface winter temperatures inferred from glycerol dialkyl glycerol tetraethers (GDGTs) along the North Icelandic shelf also record cold excursions between 1200-1900 CE, with increased sea ice cover that resulted in insulation-induced warming between c. 1550-1750 CE (Harning et al., 2019).

16
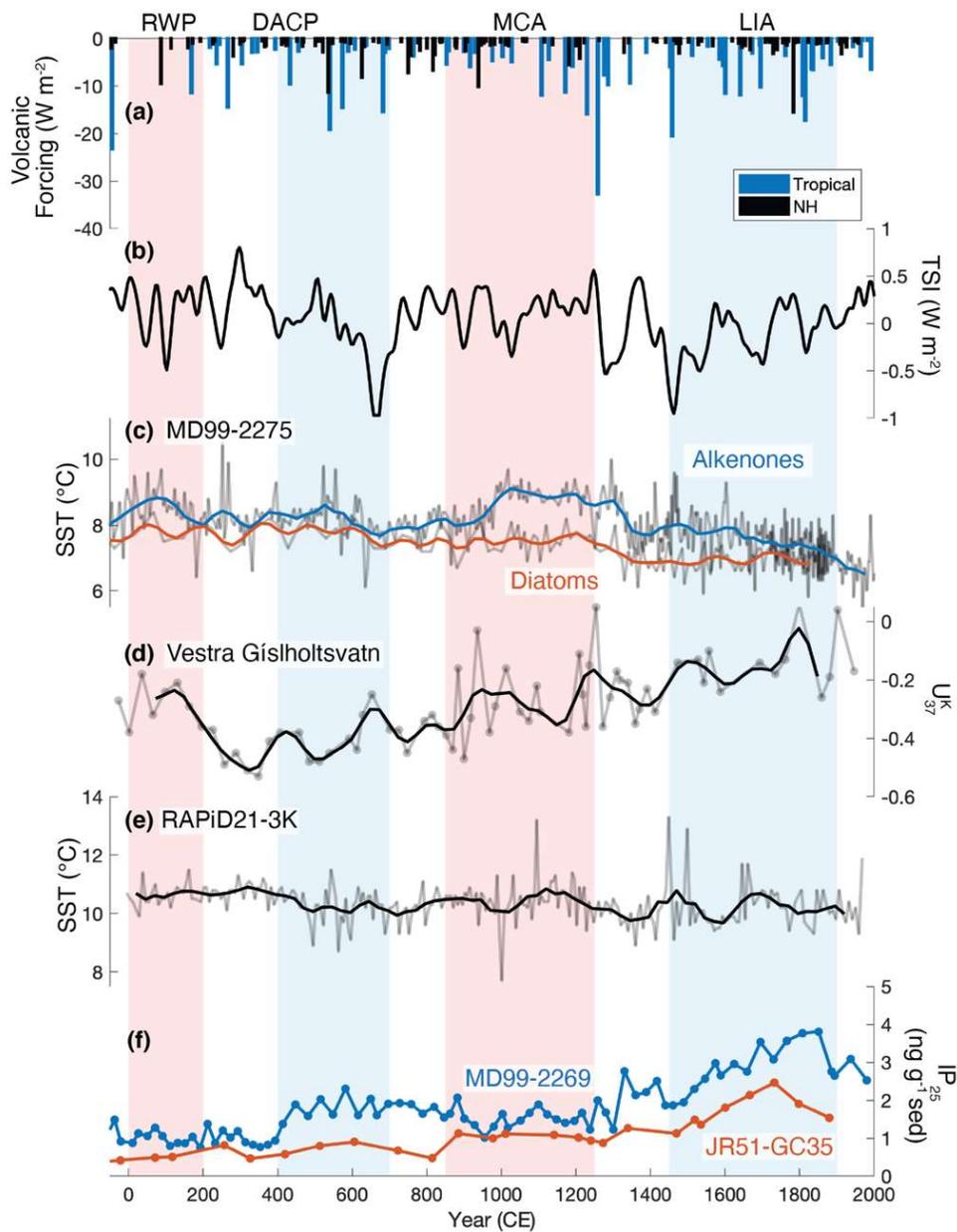
Figure 7. Major changes in radiative forcings over the past 2,000 years, including (a) volcanic forcing from tropical and NH eruptions (Sigl et al., 2015) and (b) changes in total solar irradiance (TSI; Steinhilber et al., 2009) are shown. Marine and terrestrial reconstructions from Iceland are shown, including (c) alkenone and diatom sea surface temperature (SST) reconstructions from core MD99-2275 on the North Icelandic shelf (Sicre et al., 2008; Jiang et al., 2015), (d) an alkenone winter-spring temperature reconstruction from VGHV in southwest Iceland (this study), (e) an alkenone SST record from core RAPiD21-3K in the sub-polar North Atlantic (Sicre et al., 2011), and (f) sea-ice reconstructions developed using IP$_{25}$ from cores MD99-2269 (blue) and JR51-GC35 (orange) from the North Icelandic shelf (Cabedo-Sanz et al., 2016). The timing of major climate anomalies inferred from Icelandic climate records include: the Roman Warm Period (RWP, c. 0-200 CE), Dark Ages Cold Period (c. 400-700 CE), Medieval Climate Anomaly (MCA, c. 850-1250 CE), and Little Ice Age (LIA, c. 1450-1900 CE).

17

In the VGHV record, multi-decadal variability and an inconsistent temperature response to major radiative forcings during the LIA suggest that temperature anomalies during the winter and spring are driven by both forced and unforced variability. For instance, the strong negative radiative forcing after the Samalas eruption (1258 CE) and the Wolf solar minimum (c. 1280-1350 CE) correspond to an increase in drift ice along the North Icelandic shelf (Fig. 7; Massé et al., 2008; Cabedo-Sanz et al., 2016), a cold excursion in winter subsurface temperatures from the North Icelandic shelf c. 1350-1500 CE (Harning et al 2019), and cooling in the VGHV temperature record. Similarly, the cumulative effects of the Dalton solar minimum c. 1790-1830 CE and multiple major volcanic eruptions (i.e., Laki 1783 CE, unidentified 1809 CE, and Tambora 1815 CE; Sigl et al., 2015; Toohey and Sigl, 2017) in the late 18th and early 19th century could have resulted in enhanced sea ice feedbacks and cooling in VGHV temperatures between c. 1800-1900 CE (Massé et al., 2008; Zanchettin et al., 2012; Cabedo-Sanz et al., 2016). The inconsistent response in VGHV temperatures to volcanic eruptions and solar minima between c. 1450-1750 CE could be associated with stochastic climate processes, such as the NAO, that counteracted the effects of negative radiative forcings and led to winter warming over Iceland rather than cooling.

On multi-decadal to centennial timescales, changes in the VGHV record do not consistently correspond to major temperature anomalies observed during the summer months. The differences in seasonal climate responses to external forcings imply that the regional manifestation of these events depends on the initial state of the atmosphere and ocean but is also modulated by internal climate variability (Zanchettin et al., 2012; Otto-Bliesner et al., 2016; Anchukaitis et al., 2019).

5 Conclusions

The most striking feature of the VGHV record of winter-spring temperatures is a long-term warming trend from c. 250 CE to the present. Gradual warming in cold-season temperatures is most likely driven by increasing winter and spring solar insolation over the last 2,000 years, and contrasts with inferences of mean annual and summer time warming elsewhere in the NH. On multi-decadal timescales winter-spring temperatures are sensitive to strong radiative perturbations, but regional temperature responses can be masked by internal climate variability. These processes can cause strong contrasts between winter and spring, summer, and mean annual temperatures. In general, this highlights a need for more winter and spring temperature reconstructions to improve our understanding of the magnitude and direction of cold-season temperature changes over the Common Era.

18

Appendix A

Table A1. Lake energy balance model results for air temperature perturbations.

Temperature Perturbation	Ice-off Date (Julian Day)	Water Temperature on May 1st (°C)
Control 0 °C	106 ± 9	6.6 ± 1.0
DJF -7 °C	119 ± 5	3.9 ± 2.3
DJF -3 °C	112 ± 5	6.1 ± 1.2
DJF +3 °C	93 ± 24	6.9 ± 1.0
DJF +7 °C	83 ± 30	6.9 ± 1.0
MAM -7 °C	129 ± 6	1.6 ± 1.4
MAM -3 °C	118 ± 6	4.8 ± 1.9
MAM +3 °C	95 ± 8	7.9 ± 1.0
MAM +7 °C	87 ± 8	9.6 ± 1.0
JJA -7 °C	106 ± 9	6.6 ± 1.0
JJA -3 °C	106 ± 9	6.6 ± 1.0
JJA +3 °C	106 ± 9	6.6 ± 1.0
JJA +7 °C	106 ± 8	6.6 ± 1.0
SON -7 °C	109 ± 6	6.8 ± 1.0
SON -3 °C	107 ± 6	6.7 ± 1.0
SON +3 °C	105 ± 9	6.6 ± 1.0
SON +7 °C	105 ± 9	6.7 ± 1.0

440

Table A2. Lake energy balance model results for shortwave solar radiation perturbations.

Shortwave Solar Radiation Perturbation	Ice-off Date (Julian Day)	Water Temperature on May 1st (°C)
Control	105 ± 9	6.6 ± 1.0
DJF x 0.50	108 ± 8	6.5 ± 1.0
DJF x 0.25	107 ± 8	6.5 ± 1.0
DJF x 1.25	105 ± 9	6.7 ± 1.0
DJF x 1.50	104 ± 9	6.8 ± 1.0
MAM x 0.50	124 ± 8	1.8 ± 1.6
MAM x 0.25	112 ± 9	4.5 ± 1.6
MAM x 1.25	100 ± 8	8.2 ± 1.2
MAM x 1.50	95 ± 7	9.8 ± 1.3
JJA x 0.50	106 ± 9	6.6 ± 1.0
JJA x 0.25	106 ± 9	6.6 ± 1.0
JJA x 1.25	106 ± 9	6.6 ± 1.0
JJA x 1.50	106 ± 8	6.6 ± 1.0
SON x 0.50	106 ± 8	6.5 ± 1.0
SON x 0.25	106 ± 9	6.6 ± 1.0
SON x 1.25	106 ± 8	6.6 ± 1.0
SON x 1.50	105 ± 8	6.7 ± 1.0

445   **Table A3. Lake energy balance model results for longwave radiation perturbations.**

Longwave Radiation Perturbation	Ice-off Date (Julian Day)	Water Temperature on May 1st (°C)
Control	105 ± 9	6.6 ± 1.0
-0.2 W m^{-2}	105 ± 9	6.6 ± 1.0
+0.2 W m^{-2}	105 ± 9	6.6 ± 1.0
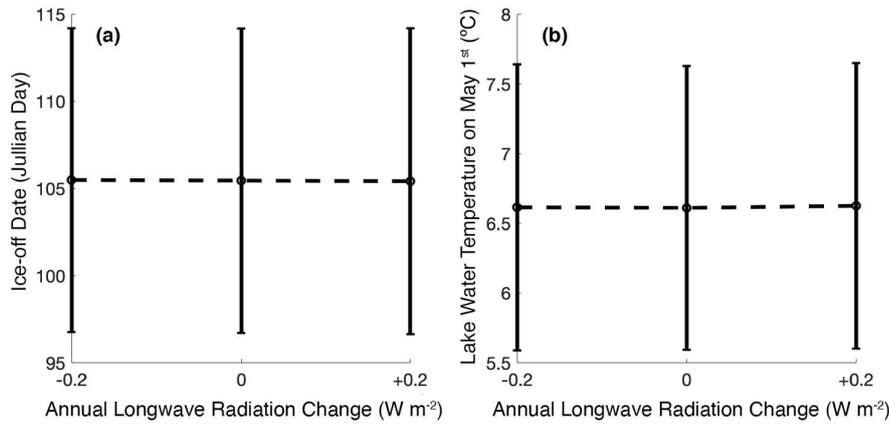
Figure A1. Lake model sensitivity tests showing the effect of annual longwave radiation perturbations on (a) ice-off dates and (b) lake water temperatures on May 1st.

450
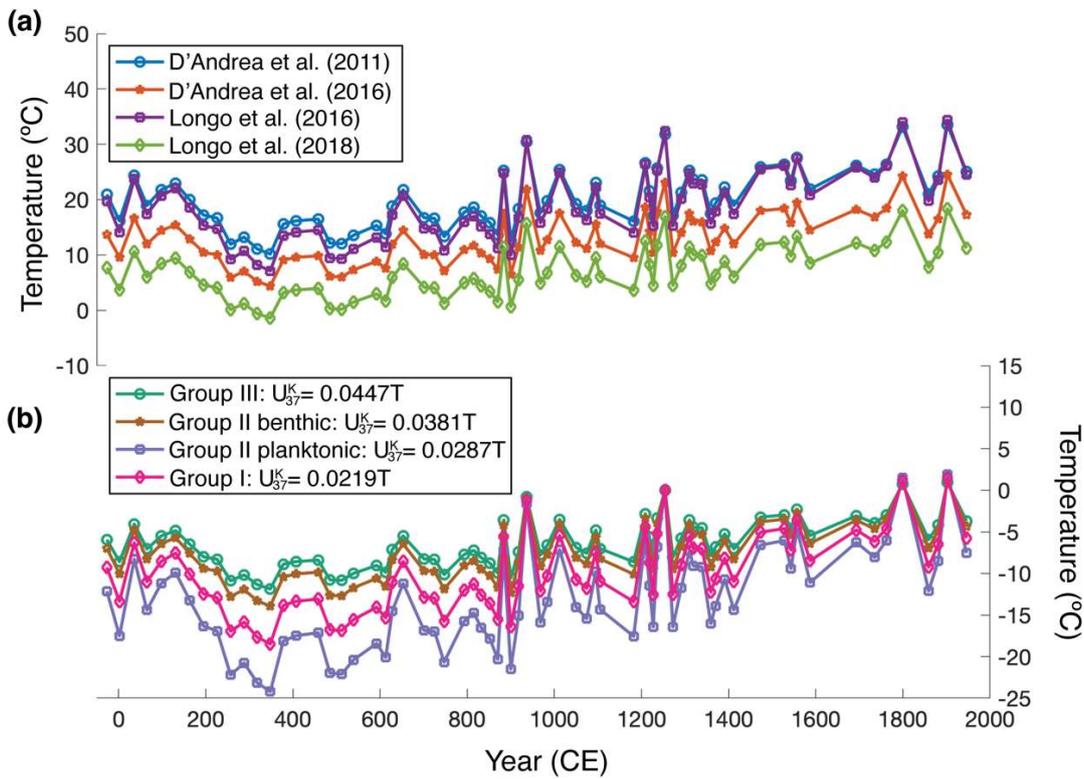
Figure A2. Alkenone calibrations from previous studies including (a) D'Andrea et al., (2011), D'Andrea et al., (2016), Longo et al., (2016), Longo et al., (2018). (b) Different temperatures calculated from slopes previously determined by D'Andrea et al., (2016) for Group III, Group II benthic, Group II planktonic, and Group I.

Data availability

Data will be made available at the National Oceanic and Atmospheric Administration National Centers for Environmental Information (NOAA NCEI) Paleoclimate Database: https://www.ncdc.noaa.gov/paleo/study/29992. The age model and information about the lake sediment core were obtained from Blair et al. (2015). Information about the lake energy balance model used in this study can be found in Dee et al. (2018) and the code for the lake energy balance model is available at: https://github.com/sylvia-dee/PRYSM. ERA-Interim daily data (1979-2019 CE) was obtained from: https://www.ecmwf.int/en/forecasts/datasets/reanalysis-datasets/era-interim (ECMWF; Dee et al., 2011). Meteorological data for southwest Iceland was obtained from: (https://en.vedur.is/climatology/data/; Icelandic Meteorological Office). Data used to make the maps in Fig. 1 can be found at: Natural Earth (https://www.naturalearthdata.com/), the National Land Survey of Iceland (https://www.lmi.is/en/), and the National Oceanic and Atmospheric Administration (NOAA) World Ocean Database (https://www.nodc.noaa.gov/OC5/WOD/pr_wod.html; Boyer et al., in preparation).

Author contributions

Study conceptualized by NR, JMR, and YH. Method development and laboratory analyses by NR and JG. NR prepared the manuscript with contributions from all co-authors.

Competing interests

The authors declare that they have no conflict of interest.

Acknowledgements

22

References

Anchukaitis, K. J., Cook, E. R., Cook, B. I., Pearl, J., D'Arrigo, R., and Wilson, R.: Coupled Modes of North Atlantic Ocean-Atmosphere Variability and the Onset of the Little Ice Age. Geophys. Res. Lett., 46, 12417-12426, https://doi.org/10.1029/2019GL084350, 2019.

Assel, R. A. and Robertson, D. M.: Changes in winter air temperatures near Lake Michigan, 1851-1993, as determined from regional lake-ice records. Limnol. Oceanogr., 40, 165-176, https://doi.org/10.4319/lo.1995.40.1.0165, 1995.

Axford, Y., Geirsdóttir, A., Miller, G.H., and Langdon, P.G.: Climate of the Little Ice Age and the past 2000 years in northeast Iceland inferred from chironomids and other lake sediment proxies. J. Paleolimnol., 41, 7-24, https://doi.org/10.1007/s10933-008-9251-1, 2009.

Axford, Y., Andresen, C.S., Andrews, J.T., Belt, S.T., Geirsdóttir, Á., Massé, G., Miller, G.H., Ólafsdóttir, S. and Vare, L.L.: Do paleoclimate proxies agree? A test comparing 19 late Holocene climate and sea-ice reconstructions from Icelandic marine and lake sediments. J. Quat. Sci., 26, 645-656, https://doi.org/10.1002/jqs.1487, 2011.

Baker, J. L., Lachniet, M. S., Chervyatsova, O., Asmerom, Y., and Polyak, V. J.: Holocene warming in western continental Eurasia driven by glacial retreat and greenhouse forcing. Nat. Geosci., 10, 430-435, https://doi.org/10.1038/ngeo2953, 2017.

Berner, K. S., Koç, N., Divine, D., Godtliebsen, F., and Moros, M.: A decadal-scale Holocene sea surface temperature record from the subpolar North Atlantic constructed using diatoms and statistics and its relation to other climate parameters. Paleoceanography, 23, https://doi.org/10.1029/2006PA001339, 2008.

Blaauw, M.: Methods and code for 'classical' age-modelling of radiocarbon sequences. Quat. Geochronol., 5, 512-518, https://doi.org/10.1016/j.quageo.2010.01.002, 2010.

Blair, C. L., Geirsdóttir, Á., and Miller, G. H.: A high-resolution multi-proxy lake record of Holocene environmental change in southern Iceland. J. Quat. Sci., 30, 281-292, https://doi.org/10.1002/jqs.2780, 2015.

Boyer, T.P., Baranova, O. K., Coleman, C., Garcia, H. E., Grodsky, A., Locarnini, R. A., Mishonov, A. V., O'Brien, T.D., Paver, C.R., Reagan, J.R., Seidov, D., Smolyar, I. V., Weathers, K., and Zweng, M. M.: World Ocean Database 2018, (in preparation).

Brassell, S. C., Eglinton, G., Marlowe, I. T., Pflaumann, U., and Sarnthein, M.: Molecular stratigraphy: a new tool for climatic assessment. Nature, 320, 129, https://doi.org/10.1038/320129a0, 1986.

Cabedo-Sanz, P., Belt, S. T., Jennings, A. E., Andrews, J. T., and Geirsdóttir, Á.: Variability in drift ice export from the Arctic Ocean to the North Icelandic Shelf over the last 8000 years: a multi-proxy evaluation. Quat. Sci. Rev., 146, 99-115, https://doi.org/10.1016/j.quascirev.2016.06.012, 2016.

Conte, M. H., Sicre, M. A., Rühlemann, C., Weber, J. C., Schulte, S., Schulz-Bull, D., and Blanz, T.: Global temperature calibration of the alkenone unsaturation index ($U_{37}^{K'}$) in surface waters and comparison with surface sediments. Geochem. Geophy. Geosy., 7, https://doi.org/10.1029/2005GC001054, 2006.

23

Coolen, M. J., Muyzer, G., Rijpstra, W. I. C., Schouten, S., Volkman, J. K., and Damsté, J. S. S.: Combined DNA and lipid analyses of sediments reveal changes in Holocene haptophyte and diatom populations in an Antarctic lake. Earth Planet. Sci. Lett., 223, 225-239, https://doi.org/10.1016/j.epsl.2004.04.014, 2004.

Cook, T. L., Bradley, R. S., Stoner, J. S., and Francus, P.: Five thousand years of sediment transfer in a high arctic watershed recorded in annually laminated sediments from Lower Murray Lake, Ellesmere Island, Nunavut, Canada. J. Paleolimnol., 41, 77, https://doi.org/10.1007/s10933-008-9252-0, 2009.

D'Andrea, W. J., and Huang, Y.: Long chain alkenones in Greenland lake sediments: Low $\delta^{13}C$ values and exceptional abundance. Org. Geochem., 36, 1234-1241, https://doi.org/10.1016/j.orggeochem.2005.05.001, 2005.

D'Andrea, W. J., Liu, Z., Alexandre, M. D. R., Wattley, S., Herbert, T. D., and Huang, Y.: An efficient method for isolating individual long-chain alkenones for compound-specific hydrogen isotope analysis. Anal. Chem., 79, 3430-3435, https://doi.org/10.1021/ac062067w, 2007.

D'Andrea, W. J., Huang, Y., Fritz, S. C., and Anderson, N. J.: Abrupt Holocene climate change as an important factor for human migration in West Greenland. Proc. Natl. Acad. Sci., 108, 9765-9769, https://doi.org/10.1073/pnas.1101708108, 2011.

D'Andrea, W. J., Vaillencourt, D. A., Balascio, N. L., Werner, A., Roof, S. R., Retelle, M., and Bradley, R. S.: Mild Little Ice Age and unprecedented recent warmth in an 1800 year lake sediment record from Svalbard. Geology, 40, 1007-1010, https://doi.org/10.1130/G33365.1, 2012.

D'Andrea, W. J., Theroux, S., Bradley, R. S., and Huang, X.: Does phylogeny control U^{K}_{37}-temperature sensitivity? Implications for lacustrine alkenone paleothermometry. Geochim. Cosmochim. Acta, 175, 168-180, https://doi.org/10.1016/j.gca.2015.10.031, 2016.

Dee, D. P., Uppala, S. M., Simmons, A. J., Berrisford, P., Poli, P., Kobayashi, S., Andrae, U., Balmaseda, M. A., Balsamo, G., Bauer, P., Bechtold, P., Beljaars, A. C. M., van de Berg, L., Bidlot, J., Bormann, N., Delsol, C., Dragani, R., Fuentes, M., Geer, A. J., Haimberger, L., Healy, S. B., Hersbach, H., Hólm, E. V., Isaksen, L., Kållberg, P., Köhler, M., Matricardi, M., McNally, A. P., Monge-Sanz, B. M., Morcrette, J. J., Park, B. K., Peubey, C., de Rosnay, P., Tavolato, C., Thépaut, J. N., and Vitart, F.: The ERA-Interim reanalysis: configuration and performance of the data assimilation system, Q. J. Roy. Meteor. Soc., 137, 553–597, https://doi.org/10.1002/qj.828, 2011.

Dee, S. G., Russell, J. M., Morrill, C., Chen, Z., and Neary, A.: PRYSM v2. 0: A Proxy System Model for Lacustrine Archives. Paleoceanogr. Paleocl., 33, 1250-1269, https://doi.org/10.1029/2018PA003413, 2018.

Delworth, T.L., Zeng, F., Vecchi, G.A., Yang, X., Zhang, L. and Zhang, R.: The North Atlantic Oscillation as a driver of rapid climate change in the Northern Hemisphere. Nature Geosci., 9, 509–512, https://doi.org/10.1038/ngeo2738, 2016.

Divine, D., Isaksson, E., Martma, T., Meijer, H.A., Moore, J., Pohjola, V., van de Wal, R.S., and Godtliebsen, F.: Thousand years of winter surface air temperature variations in Svalbard and northern Norway reconstructed from ice-core data. Polar Res., 30, 7379, https://doi.org/10.3402/polar.v30i0.7379, 2011a.

Divine, D.V., Sjolte, J., Isaksson, E., Meijer, H.A.J., Van De Wal, R.S.W., Martma, T., Pohjola, V., Sturm, C., and Godtliebsen, F.: Modelling the regional climate and isotopic composition of Svalbard precipitation using REMOiso: a comparison with available GNIP and ice core data. Hydrol. Process., 25, 3748-3759, https://doi.org/10.1002/hyp.8100, 2011b.

Eden, C. and Jung, T.: North Atlantic interdecadal variability: oceanic response to the North Atlantic Oscillation (1865–1997). J. Clim., 14, 676-691, https://doi.org/10.1175/1520-0442(2001)014<0676:NAIVOR>2.0.CO;2, 2001.

Gathorne-Hardy, F.J., Erlendsson, E., Langdon, P.G., and Edwards, K.J.: Lake sediment evidence for late Holocene climate change and landscape erosion in western Iceland. J. Paleolimnol., 42, 413-426, https://doi.org/10.1007/s10933-008-9285-4, 2009.

Geirsdóttir, Á., Miller, G.H., Thordarson, T., and Ólafsdóttir, K.B.: A 2000 year record of climate variations reconstructed from Haukadalsvatn, West Iceland. J. Paleolimnol., 41, 95-115, https://doi.org/10.1007/s10933-008-9253-z, 2009.

Geirsdóttir, Á., Miller, G.H., Andrews, J.T., Harning, D.J., Anderson, L.S., Florian, C., Larsen, D.J., and Thordarson, T.: The onset of Neoglaciation in Iceland and the 4.2 ka event. Clim. Past, 15, 25-40, https://doi.org/10.5194/cp-15-25-2019, 2019.

Haltia-Hovi, E., Saarinen, T., and Kukkonen, M.: A 2000-year record of solar forcing on varved lake sediment in eastern Finland. Quat. Sci. Rev., 26, 678-689, https://doi.org/10.1016/j.quascirev.2006.11.005, 2007.

Hanna, E., Jónsson, T., and Box, J. E.: An analysis of Icelandic climate since the nineteenth century. Int. J. Climatol.: J. Roy. Meteor. Soc., 24, 1193-1210, https://doi.org/10.1002/joc.1051, 2004.

Hanna, E., Jónsson, T., Ólafsson, J., and Valdimarsson, H.: Icelandic coastal sea surface temperature records constructed: putting the pulse on air–sea–climate interactions in the northern North Atlantic. Part I: comparison with HadISST1 open-ocean surface temperatures and preliminary analysis of long-term patterns and anomalies of SSTs around Iceland. J.Clim., 19, 5652-5666, https://doi.org/10.1175/JCLI3933.1, 2006.

Harning, D.J., Andrews, J.T., Belt, S.T., Cabedo-Sanz, P., Geirsdóttir, Á., Dildar, N., Miller, G.H. and Sepúlveda, J.: Sea Ice Control on Winter Subsurface Temperatures of the North Iceland Shelf During the Little Ice Age: A TEX$_{86}$ Calibration Case Study. Paleoceanogr. Paleoclimatol., 34, 1006-1021, https://doi.org/10.1029/2018PA003523, 2019.

Helama, S., Jones, P. D., and Briffa, K. R.: Dark Ages Cold Period: A literature review and directions for future research. Holocene, 27, 1600-1606, https://doi.org/10.1177/0959683617693898, 2017.

Hirtl, M., Stuefer, M., Arnold, D., Grell, G., Maurer, C., Natali, S., Scherllin-Pirscher, B., and Webley, P.: The effects of simulating volcanic aerosol radiative feedbacks with WRF-Chem during the Eyjafjallajökull eruption, April and May 2010. Atmos. Environ., 198, 194-206, https://doi.org/10.1016/j.atmosenv.2018.10.058, 2019.

Holmes, N., Langdon, P. G., Caseldine, C. J., Wastegård, S., Leng, M. J., Croudace, I. W., and Davies, S. M.: Climatic variability during the last millennium in Western Iceland from lake sediment records. Holocene, 26, 756-771, https://doi.org/10.1177/0959683615618260, 2016.

Hurrell, J.W.: Decadal trends in the North Atlantic Oscillation: regional temperatures and precipitation. Science, 269, 676-679, https://doi.org/10.1126/science.269.5224.676, 1995.

Icelandic Meteorological Office: https://en.vedur.is/climatology/data/, last access: 11 June 2020.

25

Isaksson, E., Divine, D., Kohler, J., Martma, T., Pohjola, V., Motoyama, H., and Watanabe, O.: Climate oscillations as recorded in Svalbard ice core $\omega^{18}O$ records between ad 1200 and 1997. Geogr. Ann. A., 87, 203-214, https://doi.org/10.1111/j.0435-3676.2005.00253.x, 2005.

580

Jiang, H., Eiríksson, J., Schulz, M., Knudsen, K.L., and Seidenkrantz, M.S.: Evidence for solar forcing of sea-surface temperature on the North Icelandic Shelf during the late Holocene. Geology, 33, 73-76, https://doi.org/10.1130/G21130.1, 2005.

Jiang, H., Muscheler, R., Björck, S., Seidenkrantz, M.S., Olsen, J., Sha, L., Sjolte, J., Eiríksson, J., Ran, L., Knudsen, K.L., and Knudsen, M.F.: Solar forcing of Holocene summer sea-surface temperatures in the northern North Atlantic. Geology, 43(3), 203-206, https://doi.org/10.1130/G36377.1, 2015.

585

Justwan, A., Koç, N., and Jennings, A.E.: Evolution of the Irminger and East Icelandic Current systems through the Holocene, revealed by diatom-based sea surface temperature reconstructions. Quat. Sci. Rev., 27, 1571-1582, https://doi.org/10.1016/j.quascirev.2008.05.006, 2008.

590

Kaufman, D. S., Schneider, D. P., McKay, N. P., Ammann, C. M., Bradley, R. S., Briffa, K. R., Miller, G.H., Otto-Bliesner, B.L., Overpeck, J.T., Vinther, B.M., and Lakes, A.: Recent warming reverses long-term Arctic cooling. Science, 325, 1236-1239, https://doi.org/10.1126/science.1173983, 2009.

Kerr, R. A.: A North Atlantic climate pacemaker for the centuries. Science, 288, 1984-1985, https://doi.org/10.1126/science.288.5473.1984, 2000.

595

Langdon, P.G., Caseldine, C.J., Croudace, I.W., Jarvis, S., Wastegård, S., and Crowford, T.C.: A chironomid-based reconstruction of summer temperatures in NW Iceland since AD 1650. Quat. Res., 75, 451-460, https://doi.org/10.1016/j.yqres.2010.11.007, 2011.

Larsen, G. and Eiríksson, J.: Late Quaternary terrestrial tephrochronology of Iceland—frequency of explosive eruptions, type and volume of tephra deposits. J. Quat. Sci., 23, 109–120, https://doi.org/10.1002/jqs.1129, 2008.

600

Larsen, D.J., Miller, G.H., Geirsdóttir, Á., and Thordarson, T.: A 3000-year varved record of glacier activity and climate change from the proglacial lake Hvítárvatn, Iceland. Quat. Sci. Rev., 30, 2715-2731, https://doi.org/10.1016/j.quascirev.2011.05.026, 2011.

Laskar, J., Robutel, P., Joutel, F., Gastineau, M., Correia, A. C. M., and Levrard, B.: A long-term numerical solution for the insolation quantities of the Earth. Astron. Astrophys., 428, 261-285, https://doi.org/10.1051/0004-6361:20041335, 2004.

605

Latif, M., Böning, C., Willebrand, J., Biastoch, A., Dengg, J., Keenlyside, N., Schweckendiek, U., and Madec, G.: Is the Thermohaline Circulation Changing?, J. Clim., 19, 4631-4637, https://doi.org/10.1175/JCLI3876.1, 2006.

Liu, Z., Zhu, J., Rosenthal, Y., Zhang, X., Otto-Bliesner, B.L., Timmermann, A., Smith, R.S., Lohmann, G., Zheng, W., and Timm, O.E.: The Holocene temperature conundrum. Proc. Natl. Acad. Sci., 111, E3501-E3505, https://doi.org/10.1073/pnas.1407229111, 2014.

26

610   Ljungqvist, F. C., Zhang, Q., Brattström, G., Krusic, P. J., Seim, A., Li, Q., Zhang, Q., and Moberg, A.: Centennial-Scale Temperature Change in Last Millennium Simulations and Proxy-Based Reconstructions, J Clim., 32, 2441-2482, https://doi.org/10.1175/JCLI-D-18-0525.1, 2019.

Longo, W. M., Theroux, S., Giblin, A. E., Zheng, Y., Dillon, J. T., and Huang, Y.: Temperature calibration and phylogenetically distinct distributions for freshwater alkenones: evidence from northern Alaskan lakes. Geochim.
615   Cosmochim. Ac., 180, 177-196, https://doi.org/10.1016/j.gca.2016.02.019, 2016.

Longo, W.M., Huang, Y., Yao, Y., Zhao, J., Giblin, A.E., Wang, X., Zech, R., Haberzettl, T., Jardillier, L., Toney, J., and Liu, Z.: Widespread occurrence of distinct alkenones from Group I haptophytes in freshwater lakes: Implications for paleotemperature and paleoenvironmental reconstructions. Earth Planet. Sci. Lett., 492, 239-250, https://doi.org/10.1016/j.epsl.2018.04.002, 2018.

620   Longo, W. M., Huang, Y., Russell, J. M., Morrill, C., Daniels, W. C., Giblin, A. E., & Crowther, J.: Insolation and greenhouse gases drove Holocene winter and spring warming in Arctic Alaska. Quaternary Science Reviews, 242, 106438, https://doi.org/10.1016/j.quascirev.2020.106438, 2020.

Mangini, A., Spötl, C., and Verdes, P.: Reconstruction of temperature in the Central Alps during the past 2000 yr from a δ^{18}O stalagmite record. Earth Planet. Sci. Lett., 235, 741-751, https://doi.org/10.1016/j.epsl.2005.05.010, 2005.

625   Marsicek, J., Shuman, B. N., Bartlein, P. J., Shafer, S. L., and Brewer, S.: Reconciling divergent trends and millennial variations in Holocene temperatures. Nature, 554, 92-96, https://doi.org/10.1038/nature25464, 2018.

Massé, G., Rowland, S. J., Sicre, M. A., Jacob, J., Jansen, E., and Belt, S. T.: Abrupt climate changes for Iceland during the last millennium: evidence from high resolution sea ice reconstructions. Earth Planet. Sci. Lett., 269, 565-569, https://doi.org/10.1016/j.epsl.2008.03.017, 2008.

630   Mauri, A., Davis, B. A. S., Collins, P. M., and Kaplan, J. O.: The climate of Europe during the Holocene: a gridded pollen-based reconstruction and its multi-proxy evaluation. Quat. Sci. Rev., 112, 109-127, https://doi.org/10.1016/j.quascirev.2015.01.013, 2015.

McKay, N. P., and Kaufman, D. S.: An extended Arctic proxy temperature database for the past 2,000 years. Sci. Data, 1, 1-10, https://doi.org/10.1038/sdata.2014.26, 2014.

635   Meyer, H., Opel, T., Laepple, T., Dereviagin, A.Y., Hoffmann, K. and Werner, M.: Long-term winter warming trend in the Siberian Arctic during the mid- to late Holocene. Nature Geosci., 8, 122–125, https://doi.org/10.1038/ngeo2349, 2015.

Miettinen, A., Divine, D., Koç, N., Godtliebsen, F., and Hall, I.R.: Multicentennial variability of the sea surface temperature gradient across the subpolar North Atlantic over the last 2.8 kyr. J. Clim. 25, 4205-4219, https://doi.org/10.1175/JCLI-D-11-00581.1, 2012.

640   Miller, G.H., Geirsdóttir, Á., Zhong, Y., Larsen, D.J., Otto-Bliesner, B.L., Holland, M.M., Bailey, D.A., Refsnider, K.A., Lehman, S.J., Southon, J.R. and Anderson, C.: Abrupt onset of the Little Ice Age triggered by volcanism and sustained by sea-ice/ocean feedbacks. Geophys. Res. Lett., 39, https://doi.org/10.1029/2011GL050168, 2012.

Moffa-Sánchez, P., Born, A., Hall, I. R., Thornalley, D. J., and Barker, S.: Solar forcing of North Atlantic surface temperature and salinity over the past millennium. Nat. Geosci., 7, 275-278, https://doi.org/10.1038/ngeo2094, 2014.

645   Moffa-Sánchez, P. and Hall, I.R.: North Atlantic variability and its links to European climate over the last 3000 years. Nat. Commun., 8, 1726, https://doi.org/10.1038/s41467-017-01884-8, 2017.

Moreno-Chamarro, E., Zanchettin, D., Lohmann, K., Luterbacher, J., and Jungclaus, J.: H. Winter amplification of the European Little Ice Age cooling by the subpolar gyre. Sci. Rep., 7, 9981, https://doi.org/10.1038/s41598-017-07969-0, 2017.

650   Moros, M., Andrews, J. T., Eberl, D. D., and Jansen, E.: Holocene history of drift ice in the northern North Atlantic: Evidence for different spatial and temporal modes. Paleoceanography, 21, https://doi.org/10.1029/2005PA001214, 2006.

Müller, P. J., Kirst, G., Ruhland, G., Von Storch, I., and Rosell-Melé, A.: Calibration of the alkenone paleotemperature index $U^{K'}_{37}$ based on core-tops from the eastern South Atlantic and the global ocean (60° N-60° S). Geochim. Cosmochim. Ac., 62, 1757-1772, https://doi.org/10.1029/2005GC001054, 1998.

655   Nakamura, H., Sawada, K., Araie, H., Suzuki, I., and Shiraiwa, Y.: Long chain alkenes, alkenones and alkenoates produced by the haptophyte alga Chrysotila lamellosa CCMP1307 isolated from a salt marsh. Org. Geochem., 66, 90-97, https://doi.org/10.1016/j.orggeochem.2013.11.007, 2014.

National Land Survey of Iceland: https://www.lmi.is/en/, last access: 24 June 2020.

Natural Earth: https://www.naturalearthdata.com/, last access: 24 June 2020.

660   Ogilvie, A. E.: The past climate and sea-ice record from Iceland, Part 1: Data to AD 1780. Clim. Change, 6, 131-152, https://doi.org/10.1007/BF00144609, 1984.

Ogilvie, A.E.J.: Documentary evidence for changes in the climate of Iceland AD 1500 to 1800, in: Climate since AD 1500, edited by: Bradley, R.S. and Jones, P.D., Routledge, London and New York, 92–117, 1992.

Ogilvie, A. E. J.: Sea-ice conditions off the coasts of Iceland AD 1601–1850 with special reference to part of the Maunder
665   Minimum period (1675–1715). AmS-Varia, 25, 9-12, 1996.

Ogilvie, A. E., Barlow, L. K., and Jennings, A. E.: North Atlantic climate c. AD 1000: Millennial reflections on the Viking discoveries of Iceland, Greenland and North America. Weather, 55, 34-45, https://doi.org/10.1002/j.1477-8696.2000.tb04028.x, 2000.

Ogilvie, A. E., and Jónsson, T.: "Little Ice Age" research: A perspective from Iceland. Clim. Change, 48, 9-52,
670   https://doi.org/10.1007/978-94-017-3352-6_1, 2001.

Ojala, A. E., and Alenius, T.: 10,000 years of interannual sedimentation recorded in the Lake Nautajärvi (Finland) clastic–organic varves. Palaeogeogr., Palaeoclimatol., Palaeoecol., 219, 285-302, https://doi.org/10.1016/j.palaeo.2005.01.002, 2005.

Ólafsdóttir, S., Jennings, A. E., Geirsdóttir, Á., Andrews, J., and Miller, G. H.: Holocene variability of the North Atlantic
675   Irminger current on the south-and northwest shelf of Iceland. Mar. Micropaleontol., 77, 101-118, https://doi.org/10.1016/j.marmicro.2010.08.002, 2010.

Oman, L., Robock, A., Stenchikov, G. L., Thordarson, T., Koch, D., Shindell, D. T., and Gao, C.: Modeling the distribution of the volcanic aerosol cloud from the 1783–1784 Laki eruption. J. Geophys. Res.: Atmos., 111, https://doi.org/10.1029/2005JD006899, 2006.

680   Ono, M., Sawada, K., Shiraiwa, Y., and Kubota, M.: Changes in alkenone and alkenoate distributions during acclimatization to salinity change in Isochrysis galbana: Implication for alkenone-based paleosalinity and paleothermometry. Geochem. J., 46, 235-247, https://doi.org/10.2343/geochemj.2.0203, 2012.

Opel T., Laepple T., Meyer H., Dereviagin A.Y., and Wetterich S.: Northeast Siberian ice wedges confirm Arctic winter warming over the past two millennia. Holocene, 27, 1789-1796, https://doi.org/10.1177/0959683617702229, 2017.

685   Orme, L.C., Miettinen, A., Divine, D., Husum, K., Pearce, C., Van Nieuwenhove, N., Born, A., Mohan, R. and Seidenkrantz, M.S.: Subpolar North Atlantic sea surface temperature since 6 ka BP: Indications of anomalous ocean-atmosphere interactions at 4-2 ka BP. Quat. Sci. Rev., 194, 128-142, https://doi.org/10.1016/j.quascirev.2018.07.007, 2018.

Otto-Bliesner, B. L., Brady, E. C., Fasullo, J., Jahn, A., Landrum, L., Stevenson, S., Rosenbloom, N., Mai, A., and Strand, G.: Climate variability and change since 850 CE: An ensemble approach with the Community Earth System Model. B.Am.
690   Meteorol. Soc., 97, 735-754, https://doi.org/10.1175/BAMS-D-14-00233.1, 2016.

PAGES 2K Consortium: Continental-scale temperature variability during the past two millennia. Nat. Geosci., 6, 339-346, https://doi.org/10.1038/ngeo1797, 2013.

PAGES 2K Consortium: Consistent multi-decadal variability in global temperature reconstructions and simulations over the Common Era. Nat. Geosci., 12, 643-649, https://doi.org/10.1038/s41561-019-0400-0, 2019.

695   Pla, S., and Catalan, J.: Chrysophyte cysts from lake sediments reveal the submillennial winter/spring climate variability in the northwestern Mediterranean region throughout the Holocene. Clim. Dyn., 24, 263-278, https://doi.org/10.1007/s00382-004-0482-1, 2005.

Prahl, F. G., and Wakeham, S. G.: Calibration of unsaturation patterns in long-chain ketone compositions for palaeotemperature assessment. Nature, 330, 367, https://doi.org/10.1038/330367a0, 1987.

700   Prahl, F. G., Muehlhausen, L. A., and Zahnle, D. L.: Further evaluation of long-chain alkenones as indicators of paleoceanographic conditions. Geochim. Cosmochim. Ac., 52, 2303-2310, https://doi.org/10.1016/0016-7037(88)90132-9, 1998.

Ran, L., Jiang, H., Knudsen, K.L. and Eiríksson, J.: Diatom-based reconstruction of palaeoceanographic changes on the North Icelandic shelf during the last millennium. Palaeogeogr., Palaeoclimatol., Palaeoecol., 302, 109-119,
705   https://doi.org/10.1016/j.palaeo.2010.02.001, 2011.

Rehfeld, K., Trachsel, M., Telford, R. J., and Laepple, T.: Assessing performance and seasonal bias of pollen-based climate reconstructions in a perfect model world. Clim. Past, 12, 2255-2270, https://doi.org/10.5194/cp-12-2255-2016, 2016.

Richter, N., Longo, W. M., George, S., Shipunova, A., Huang, Y., and Amaral-Zettler, L.: Phylogenetic diversity in freshwater-dwelling Isochrysidales haptophytes with implications for alkenone production. Geobiology, 17, 272-280,
710   https://doi.org/10.1111/gbi.12330, 2019.

Salacup, J. M., Farmer, J. R., Herbert, T. D., and Prell, W. L.: Alkenone Paleothermometry in Coastal Settings: Evaluating the Potential for Highly Resolved Time Series of Sea Surface Temperature. Paleoceanogr. Paleoclimatol., 34, 164-181, https://doi.org/10.1029/2018PA003416, 2019.

Schmidt, G. A., Jungclaus, J. H., Ammann, C. M., Bard, E., Braconnot, P. C. T. J. D. G., Crowley, T. J., Delaygue, G., Joos, F., Krivova, N.A., Muscheler, R., and Otto-Bliesner, B. L.: Climate forcing reconstructions for use in PMIP simulations of the last millennium (v1. 0). Geosci. Model Devel., 4, 33-45, https://doi.org/10.5194/gmd-4-33-2011, 2011.

Sicre, M.A., Jacob, J., Ezat, U., Rousse, S., Kissel, C., Yiou, P., Eiríksson, J., Knudsen, K.L., Jansen, E., and Turon, J.L.: Decadal variability of sea surface temperatures off North Iceland over the last 2000 years. Earth Planet. Sci. Lett., 268, 137-142, https://doi.org/10.1016/j.epsl.2008.01.011, 2008.

Sicre, M.A., Hall, I.R., Mignot, J., Khodri, M., Ezat, U., Truong, M.X., Eiríksson, J., and Knudsen, K.L.: Sea surface temperature variability in the subpolar Atlantic over the last two millennia. Paleoceanography, 26, https://doi.org/10.1029/2011PA002169, 2011.

Sigl, M., Winstrup, M., McConnell, J.R., Welten, K.C., Plunkett, G., Ludlow, F., Büntgen, U., Caffee, M., Chellman, N., Dahl-Jensen, D., and Fischer, H.: Timing and climate forcing of volcanic eruptions for the past 2,500 years. Nature, 523, 543-549, https://doi.org/10.1038/nature14565, 2015.

Steinhilber, F., Beer, J., and Fröhlich, C.: Total solar irradiance during the Holocene. Geophys. Res. Lett., 36, https://doi.org/10.1029/2009GL040142, 2009.

Sun, Q., Chu, G., Liu, G., Li, S., and Wang, X.: Calibration of alkenone unsaturation index with growth temperature for a lacustrine species, Chrysotila lamellosa (Haptophyceae). Org. Geochem., 38, 1226-1234, https://doi.org/10.1016/j.orggeochem.2007.04.007, 2007.

Theroux, S., D'Andrea, W. J., Toney, J., Amaral-Zettler, L., and Huang, Y.: Phylogenetic diversity and evolutionary relatedness of alkenone-producing haptophyte algae in lakes: implications for continental paleotemperature Earth Planet. Sci. Lett., 300, 311-320, https://doi.org/10.1016/j.epsl.2010.10.009, 2010.

Theroux, S., Toney, J., Amaral-Zettler, L., and Huang, Y.: Production and temperature sensitivity of long chain alkenones in the cultured haptophyte Pseudoisochrysis paradoxa. Org. Geochem., 62, 68-73, https://doi.org/10.1016/j.orggeochem.2013.07.006, 2013.

Thornalley, D., Elderfield, H. and McCave, I.: Holocene oscillations in temperature and salinity of the surface subpolar North Atlantic. Nature, 457, 711–714, https://doi.org/10.1038/nature07717, 2009.

Toohey, M., and Sigl, M.: Volcanic stratospheric sulphur injections and aerosol optical depth from 500 BCE to 1900 CE. Earth Syst. Sci. Data, 9, 809-831, https://doi.org/10.5194/essd-9-809-2017, 2017.

Toney, J. L., Huang, Y., Fritz, S. C., Baker, P. A., Grimm, E., and Nyren, P.: Climatic and environmental controls on the occurrence and distributions of long chain alkenones in lakes of the interior United States. Geochim. Cosmochim. Ac., 74, 1563-1578, https://doi.org/10.1016/j.gca.2009.11.021, 2010.

745 Toney, J. L., Theroux, S., Andersen, R. A., Coleman, A., Amaral-Zettler, L., and Huang, Y.: Culturing of the first 37: 4 predominant lacustrine haptophyte: geochemical, biochemical, and genetic implications. Geochim. Cosmochim. Ac., 78, 51-64, https://doi.org/10.1016/j.gca.2011.11.024, 2012.

Van Nieuwenhove, N., Pearce, C., Knudsen, M. F., Røy, H., and Seidenkrantz, M. S.: Meltwater and seasonality influence on subpolar Gyre circulation during the Holocene. Palaeogeogr., Palaeoclimatol., Palaeoecol., 502, 104-118, https://doi.org/10.1016/j.palaeo.2018.05.002, 2018.

750 Visbeck, M., Chassignet, E. P., Curry, R. G., Delworth, T. L., Dickson, R. R., and Krahmann, G.: The ocean's response to North Atlantic Oscillation variability. Geophys. Monogr. Sr., 134, 113-146, https://doi.org/10.1029/134GM06, 2003.

Wang, Z., and Liu, W.: Calibration of the $U_{37}^{K'}$ index of long-chain alkenones with the in-situ water temperature in Lake Qinghai in the Tibetan Plateau. Chinese Sci. Bull., 58, 803-808, https://doi.org/10.1007/s11434-012-5527-y, 2013.

Wang, J., Yang, B., Ljungqvist, F. C., Luterbacher, J., Osborn, T. J., Briffa, K. R., and Zorita, E.: Internal and external forcing 755 of multidecadal Atlantic climate variability over the past 1,200 years. Nature Geosci., 10, 512-517, https://doi.org/10.1038/ngeo2962, 2017.

Yao, Y., Zhao, J., Longo, W.M., Li, G., Wang, X., Vachula, R.S., Wang, K.J. and Huang, Y.: New insights into environmental controls on the occurrence and abundance of Group I alkenones and their paleoclimate applications: Evidence from volcanic lakes of northeastern China. Earth Planet. Sci. Lett., 527, https://doi.org/10.1016/j.epsl.2019.115792, 2019.

760 Yeager, S. G., and Robson, J. I.: Recent progress in understanding and predicting Atlantic decadal climate variability. Curr. Clim. Change Rep., 3, 112-127, https://doi.org/10.1007/s40641-017-0064-z, 2017.

Zanchettin, D., Timmreck, C., Graf, H.F., Rubino, A., Lorenz, S., Lohmann, K., Krüger, K. and Jungclaus, J.H.: Bi-decadal variability excited in the coupled ocean–atmosphere system by strong tropical volcanic eruptions. Clim. Dyn., 39, 419-444, https://doi.org/10.1007/s00382-011-1167-1, 2012.

765 Zheng, Y., Huang, Y., Andersen, R. A., and Amaral-Zettler, L. A.: Excluding the di-unsaturated alkenone in the U_{37}^{K} index strengthens temperature correlation for the common lacustrine and brackish-water haptophytes. Geochim. Cosmochim. Ac., 175, 36-46, https://doi.org/10.1016/j.gca.2015.11.024, 2016.

Zink, K. G., Leythaeuser, D., Melkonian, M., and Schwark, L.: Temperature dependency of long-chain alkenone distributions in recent to fossil limnic sediments and in lake waters. Geochim. Cosmochim. Ac., 65, 253-265, 770 https://doi.org/10.1016/S0016-7037(00)00509-3, 2001.